Electron tunneling through water layer in nanogaps probed by plasmon resonances

Tatiana V. Teperik,[1,*] Andrey K. Kazansky,[1,2,3] and Andrei G. Borisov[4,†]
[1]*Donostia International Physics Center, Aptdo. 1072, 20080 San Sebastian, Spain*
[2]*Materials Physics Center CSIC-UPV/EHU and Donostia International Physics Center DIPC, Paseo Manuel de Lardizabal 5, 20018 Donostia-San Sebastián Spain*
[3]*IKERBASQUE, Basque Foundation for Science, E-48011 Bilbao, Spain*
[4]*Institut des Sciences Moléculaires d'Orsay, UMR 8214 CNRS-Université Paris-Sud, Bâtiment 351, 91405 Orsay Cedex, France*
(Received 2 February 2016; published 25 April 2016)

With an example of the periodic plasmonic dolmen structure we performed a theoretical study of the effect of the conducting water layer on the plasmon resonances of the system with narrow gaps. Using the scanning tunneling microscopy studies of the conductance of the water junctions as inputs, we show that water layer(s) should affect plasmon modes of the systems with nm and sub nm gaps in two ways. The frequency of the plasmon modes shifts because of the dielectric screening, as commonly used in plasmonic sensors, and the corresponding resonance in the optical spectra looses intensity and broadens because of the resistive tunneling current. The water layer in the junction lowers potential barrier for electron tunneling, so that quantum effects in plasmon response appear for the junction width at least twice larger as compared to the vacuum gaps.

DOI: 10.1103/PhysRevB.93.155431

I. INTRODUCTION

The coupling between the incident electromagnetic radiation and collective electronic excitations in metallic nanoparticles, plasmons, allows one to resonantly enhance the optical response and to engineer the enhanced near fields at the nm scale. Owing to the applied and fundamental interest with a broad plethora of phenomena linked with plasmon excitations, plasmonics nowadays is at the focus of intense research interest [1–5]. The fast development of the field is to a large extent due to the the technological progress, which made it possible to engineer nanostructures with sought plasmon and optical properties [5–8].

Among various geometries, the nanostructures with narrow gaps between nanoparticles such as plasmon dimer are of particular interest because of the extremely large localized fields produced by the interaction between the charges of opposite sign across the gap. Along with field enhancement, e.g., spherical dimer geometry leads to strong coupling between the plasmon modes of individual nanoparticles leading to the frequency shift of the plasmon resonances of the dimer [1,2,8–11]. These effects are used in sensing [5,12,13], plasmon ruler [14,15], and nonlinear applications [16–18] among others. Recently, it has been demonstrated that when the gap size is reduced to some nm range and below, quantum effects due to the nonlocal screening and electron tunneling emerge [19,20]. The so-called quantum tunneling regime in gap plasmonics was addressed in a number of theoretical works, and it was demonstrated experimentally [18,20–29]. Account for electron tunneling in optical properties of nanostructures with narrow gaps removes the nonphysical divergence of the electric fields and energy shifts of the plasmon modes inherent to the classical electromagnetic theory [10], and it restores the smooth transition from separated to contacted objects [30]. The quantum tunneling regime provides new functionalities that can be used to control plasmon devices [31].

Most of the full quantum calculations reported so far considered vacuum gaps between nanoobjects. At the same time, the existing experimental studies of optical response of the systems with narrow gaps have been essentially performed in ambient conditions, which results in the presence of adsorbed water layers and, therefore water filling of the sub-nm gaps. From the scanning tunneling microscopy (STM) and break junction studies [32–37] it is known that the presence of water in the STM junction substantially increases the conductance of the latter. To attain the electron tunneling currents observed for 1 nm wide wet junctions, it might require at least twice smaller width of the junction in the ultrahigh vacuum conditions.

The present paper aims to answer the question: How does the presence of water in plasmonic gaps alter the quantum effects in optical response? To this end we used the STM conductance data to model the dielectric properties of the thin water junctions and performed quantitative study of the light scattering on periodic array of plasmonic dolmen structures (Fig. 1) with and without a water layer in the gap between nanorods. We show that the effect of the water layer in the tunneling gaps with the width less than 2 nm is twofold. First, the frequency of the bonding plasmon resonance redshifts because of the dielectric screening, the effect which is widely used in the plasmon sensor applications [5,12,13]. Second, the resonance broadens because of the resistive losses associated with tunneling current [18,30]. We compare our results with existing model calculations of the effect of plasmonic gaps functionalized with conducting self-assembled molecular layers (SAMs). We also discuss the possible use of the device for the sensing applications.

The paper is organized as follows. The geometry of the system and the theoretical approach used in our study is described in Sec. I. Section II presents the results and their discussion. Finally, the major conclusions are summarized in Sec. III.

*tatiana.teperik@u-psud.fr
†andrei.borissov@u-psud.fr

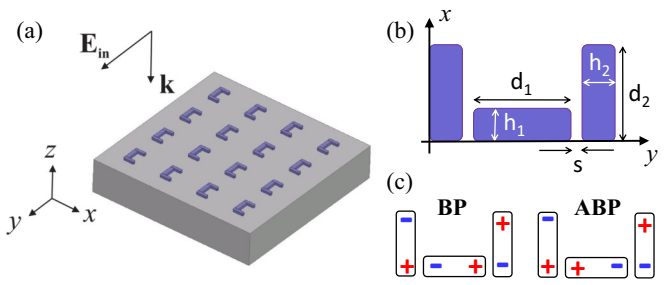

FIG. 1. (a) Schematic representation of the periodic plasmonic dolmen structure illuminated by the plane wave incident perpendicular to the surface. (b) Sketch of the geometry of the individual nanodolmen. (c) Sketch of the plasmon induced charge distribution for the bonding plasmon mode (BP) and antibonding plasmon mode (ABP) of the nanodolmen excited by the incident plane wave polarized along the y axis.

II. GEOMETRY AND THEORETICAL APPROACH

To demonstrate the effect of the water layer(s) in narrow plasmonic gaps, and to study the possibility of the sensing applications, we investigate the scattering of electromagnetic radiation by the periodic nanoantenna arrays. Each individual nanoantenna is represented by the gold nanoparticle dolmen-type structure, i.e., a dimer formed by the two parallel dipole rods oriented along the x axis with an orthogonal third dipole rod oriented along the y axis and placed in the gap of the dimer as we show in Fig. 1. We used a symmetric dolmen with geometry characterized by the lengths of the rods d_1 and d_2, their widths h_1 and h_2, their height with respect to the substrate plane H (we used the same height for all nanorods), and the width of the plasmonic gap s (see Fig. 1). The nanoparticle corners are smoothed with typical radius of curvature $r =$ 6 nm in order to avoid the electromagnetic field singularity on one side and to be close to realistic plasmonic structures available with modern nanofabrication facilities. The rods are located on a glass substrate and form a rectangular periodic array with period T. We consider illumination by a normally incident light with electric field polarized along the y axis.

The plasmon modes of the dolmen-type structures have been studied in great detail in literature [38–40]. The present choice of polarization of the incident light allows excitation of the bonding (BP) and antibonding (ABP) plasmon modes with distribution of the plasmon induced charges sketched in Fig. 1. The BP corresponds to the plasmon induced charges of opposite sign across the gap s. This leads to the enhanced fields in the gap regions and strong coupling between the dipolar plasmon modes localised on each individual nanorod [8]. Therefore, the BP is expected to show the highest sensitivity to the change of the character of the gap such as dielectric screening and conductivity. The structure parameters are set such that the wavelength of the BP is larger than the diffraction threshold value at normal incidence for the studied array: $d_1 = 146$ nm, $d_2 = 126$ nm, $h_1 = 46$ nm, $h_2 =$ 33 nm, $H = 30$ nm, and $T = 466$ nm. This allows us to avoid the complication of the analysis of the results because of the presence of diffracted beams and threshold anomalies [41] and to focus the discussion on the effect of the water presence in the plasmonic gap.

The scattering of electromagnetic radiation by the periodic array of nanodolmens is calculated with finite element solver of classical Maxwell equations as implemented in the COMSOL package [42]. The Johnson and Christy data [43] for the frequency-dependent dielectric function of gold nanorods has been used. To reveal the effect of the electron tunneling through the water layer on optical response we consider both: the case of the vacuum gap between nanorods and the case of the gap containing the water layer. For the widths of the gap $s \geqslant 0.7$ nm addressed here, the electron tunneling through the vacuum gap between gold surfaces is negligible [30,44]. The vacuum gap is thus described via classical dielectric constant $\varepsilon_g = 1$. The possible effect of nonlocality will be discussed below in this paper.

To model the effect of the electron tunneling through water on the optical properties of the system we assume that the water is present only in the gap region. Thus, along with study of quantum effects, we also test the ability of the structure to detect the presence of tiny amounts of water. The linear response theory allows one to relate the optical potential across the junction $\mathrm{V}_\omega = s\mathrm{E}_\omega$ and the ac current density through the junction at optical frequencies. Here E_ω is the electric field in the junction oscillating at optical frequency ω. The dissipative component (in phase with the driving field) of the ac current density through the junction is given by [45,46]:

$$J_\omega(s) = \frac{\mathrm{V}_\omega}{2\omega}[J_{\mathrm{dc}}(\mathrm{U}+\omega,s) - J_{\mathrm{dc}}(\mathrm{U}-\omega,s)]. \qquad (1)$$

U is the applied dc bias, and $J_{\mathrm{dc}}(\mathrm{U} \pm \omega)$ is the dc current at dc bias $\mathrm{U} \pm \omega$. In our case $\mathrm{U} = 0$, and assuming the slow variation of J_{dc} with U, we obtain the classical limit $J_\omega(s) = sG(s)\mathrm{E}_\omega$, where $G(s) = dJ_{\mathrm{dc}}(\mathrm{U},s)/d\mathrm{U}$ is the dc conductance of the junction. Thus, to model the effect of the electron tunneling through water on the optical properties of the system we represent the water layer in the gap using a permittivity

$$\varepsilon_g = \varepsilon_\infty + i\frac{4\pi\sigma}{\omega}, \qquad (2)$$

where $\sigma = sG(s)$ is the conductivity, and $\varepsilon_\infty = 1.8$ is the electronic contribution to the dielectric function of water.

Assuming the typical exponential dependence of the conductance of the tunneling junction on its width, we set the conductivity σ of the water layer of width s as:

$$\sigma = sG_{\max}\exp[-\gamma s]. \qquad (3)$$

The parameters $G_{\max}$ and γ can be directly extracted from the available experimental studies of the conductance of water junctions performed with STM or break junction techniques [32–37]. The dependence of the tunneling current on the width of the junction is typically analyzed using the semiclassical approach for the electron tunneling through the rectangular barrier, where $\gamma = 10.12\ \mathrm{eV}^{-1/2}\ \mathrm{nm}^{-1}\sqrt{\Phi}$. The effective height of the tunneling barrier Φ extracted from these studies varies within the range of 0.2–1.5 eV for gold electrodes. This is to be compared with 4–5 eV barrier for the vacuum junctions. The strong reduction of the tunneling barrier due to the presence of water has been confirmed by the theoretical studies [47–49] albeit attributed to various effects such as presence of the resonant electron states and transport properties of the electrons in the conduction band of water. Consistent with

recent STM data [32,33], we set $\gamma = 5.5\ \mathrm{nm}^{-1}$ (corresponding to effective barrier $\Phi = 0.3$ eV). The $G_{\max}$ parameter has been set equal to $G_{\max} = 0.08 G_0$ ($G_0 = 77\,\mu$s is the quantum of conductance) as can be obtained from the STM conductance curves under assumption that the current flows through the area with diameter $D \simeq 1$ Å. This is supported by the formation of the single atom contact (conductance G_0) at the width of the gap $s = 0$. It is worth it to mention that variation of $G_{\max}$ by a factor of 3 would roughly correspond to the change of the gap width s by 0.2 nm, which would not affect the main conclusions of our study. Provided definition of the numerical values of the parameters presented above, the permittivity of the water layer used in our calculation has been taken as:

$$\varepsilon_g = 1.8 + i163\frac{s}{\omega}\exp[-5.5s], \tag{4}$$

where the gap width s is measured in nm and frequency ω is measured in eV.

III. RESULTS AND DISCUSSION

First, we analyze the dependence of the reflectance spectra of the periodic array of nanodolmens on the geometry of the individual nanoparticle. The results shown in Fig. 2 and in Fig. 3 have been obtained for the vacuum gap between nanorods. The light with polarization parallel to the y axis excites the localized dipolar plasmon resonance of the y-oriented nanorod, while the dipolar plasmon modes of the two x-oriented rods are excited trough the near-field interaction. The coupling between the individual nanorods forms the low-energy BP mode of the dolmen with distribution of electric fields shown in Fig. 2. The fields are strongly enhanced in the gaps with an enhancement factor close to 500 in this case. As we already pointed out, the enhanced fields created by the plasmon induced screening charges of opposite sign across the gap, make the BP mode particularly sensitive to the eventual presence of the water layer in the gaps. The excitation of the BP mode of the dolmen is manifested in the reflectance spectra of the periodic array by a pronounced peak in near infrared. Since the resonance wavelength is larger than the diffraction threshold of the grating, for the normal incidence geometry used here only the reflection/transmission along the z axis perpendicular to the surface of the grating is possible.

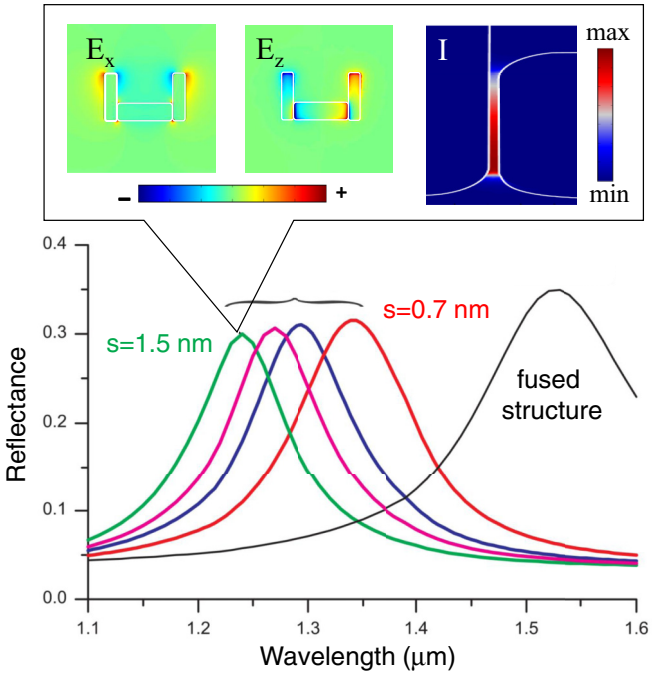

FIG. 2. Reflectance spectra of the periodic array as function of the size of plasmonic gap s. From the left spectrum to the right spectrum: $s = 1.5$ nm (green), $s = 1.2$ nm (magenta), $s = 1.$ nm (blue), and $s = 0.7$ nm (red). The reflectance of the fused ($s = 0$) Π-type structure is shown with the black curve. At the top of the figure we plot the near field components E_x and E_z, and near field intensity I calculated at the reflectance maximum of the $s = 1.5$ nm structure. The E_x and I are presented in the (xy) plane passing through the middle of the rods. The E_z is presented in the (xy) plane located 3 nm above the structure.

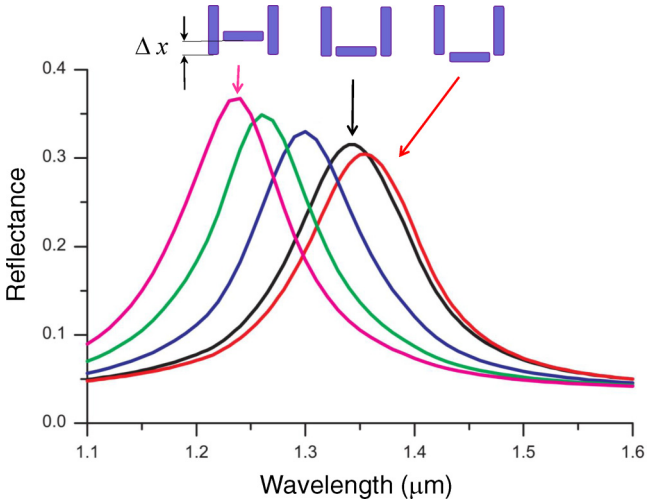

FIG. 3. Reflectance spectra of the periodic array of nanodolmens with $s = 0.7$ nm gaps. Results are shown for different values of the displacement of the the central rod along the x axis, Δx. From the left spectrum to the right spectrum: $\Delta x = 30$ nm (magenta), $\Delta x = 20$ nm (green), $\Delta x = 10$ nm (blue), $\Delta x = 0$ nm (black), $\Delta x = -10$ nm (red). The evolution of the geometry is sketched at the top of the figure.

The dependence of the BP resonance on the width of the gap s is shown in Fig. 2. With decreasing s the coupling between plasmon modes localised on individual nanorods increases and the BP resonance shifts to longer wavelengths. In the present case the gap is formed by the flat portions of metallic surface (flat capacitor). Then, opposite to the case of plasmon dimer formed by spherical nanoparticles, the fields in the junction, and the redshift of the BP resonance calculated with classical electrodynamics is not diverging with $s \to 0$ [50–53]. The reflectance spectra of the dolmen smoothly evolves into that of the fused Π-type structure at $s = 0$. The change of the width of the gap from 1.5 nm to 0 is associated with increase of the resonance wavelength by 0.3 μm.

The dependence of the BP resonance on the displacement of the central rod along the x axis is illustrated in Fig 3. The reflection spectra are shown for different values of the displacement Δx from the initial position corresponding to the perfect alignment geometry shown in Fig. 1. The Δx is defined at the inset of the figure. The calculations have been

performed for the width of the gap $s = 0.7$ nm. Large positive Δx, corresponds to the central rod positioned deep inside the dimer formed by the two parallel rods. The field enhancement and the Coulomb interaction between the charges localized at extremities of the dipole antennas becomes smaller and the BP resonance is moved towards the short wavelength. Decreasing Δx (evolution towards aligned geometry) leads to the larger coupling between plasmon modes of individual nanorods and the BP redshifts up to small negative Δx. Obviously, large negative displacement (not shown) would finally separate the plasmon induced charges and lead to the blueshift of the resonance. For negative Δx the contact area between the flat surfaces across the gap decreases which will lead to smaller tunneling current trough the gap. Therefore, we have chosen to perform the calculations with a water layer in the gap for the $\Delta x = 0$ geometry allowing good compromise between the field enhancement and tunneling efficiency of the gap.

As follows from the STM and break junction experiments [32–37], in the case when the water layer is present in the junction, the electron tunneling becomes important for the width of the gap below 2 nm. For comparison, to observe the change of the plasmon response because of the electron tunneling between the gold surfaces separated by the vacuum gap would require $s < 0.5$ nm [30,44]. To study the effect of water on the optical response we compare results of the three calculations: (i) assuming vacuum gap with $\varepsilon_g = 1$; (ii) using $\varepsilon_g = 1.8$ so that only the dielectric screening of water is accounted for; (iii) using the dielectric function of the gap given by Eq. (4). This latter choice allows us to incorporate both the dielectric screening and tunneling effect because of the presence of the water layer. The reflectance spectra of the periodic dolmen structure calculated with dielectric properties of the gap set according to models (i), (ii), and (iii) are shown in Fig. 4. Calculations are performed for the widths of the gap $s = 0.7$ nm, $s = 1.0$ nm, $s = 1.5$ nm, as indicated at the top of the corresponding panels of the figure. This corresponds to 2, 3, and 4 layers of water molecules, respectively [32,47].

Comparison between the reflectance spectra in Fig. 4 calculated for the vacuum gaps [model (i)] and for the dielectric gaps [model (ii)] shows that the presence of the dielectric (here water) in the junction leads to a significant shift of the plasmon resonance to the longer wavelength. This shift can be related to the shift of the cavity eigenmode [54], and it is used in plasmon sensor applications [5,12,13]. For the range of the widths of plasmonic gaps s encompassed in our study the change of the resonance wavelength produced by the change of the dielectric constant of the gap shows only weak dependence on s. When the electron tunneling through the water layer is accounted for [model (iii)] the BP mode of the dolmen and so the reflectance spectrum is affected already for the 1.5 nm wide gap. The smaller is the width of the gap, the stronger is the effect. Primarily, the tunneling leads to the broadening of the BP resonance because of resistive losses [18,30]. For the narrowest gap $s = 0.7$ nm, the tunneling current is large enough so that along with resonance broadening, the BP shifts to larger wavelength as compared to the calculation (ii) which takes into account only the dielectric screening in water. The shift of the wavelength of the BP mode reflects its evolution to the plasmon resonance of the fully metallic Π-type structure. Indeed, because of the electron tunneling the nanorods appear conductively coupled prior to the direct geometrical contact. Thus, the presence of the water layer in the gap has two effects: redshift and broadening of the plasmon resonances of the structure.

It is important to stress that the change of the optical properties because of the electron tunneling effect in the case of the flat gap geometry considered here is very different from the spherical dimer case. For the spherical dimer characterized by the classical divergence of the fields for $s = 0$ [10], the weak tunneling through molecular layer in narrow junctions leads to the blueshift of the bonding dipole plasmon [55–57]. When the tunneling through the gap becomes strong, the bonding modes of the capacitively coupled dimer progressively disappear, the field enhancement in the middle of the junction is quenched, and the charge transfer modes of the conductively coupled structure emerge [18,20,24,25,30]. According to our results, and consistent with experimentally determined conductances of the water and vacuum gold-gold junctions [32–37], the strong tunneling effects for the spherical dimer should appear for the 1.2 nm wide water filled gaps. This is to be compared with 0.3–0.5 nm as reported for vacuum gaps [18,25,30]. The disappearance of the bonding dipole mode of the spherical dimer, instead of the strong redshift towards the modes of the fused structure as calculated here for the nanodolmen array,

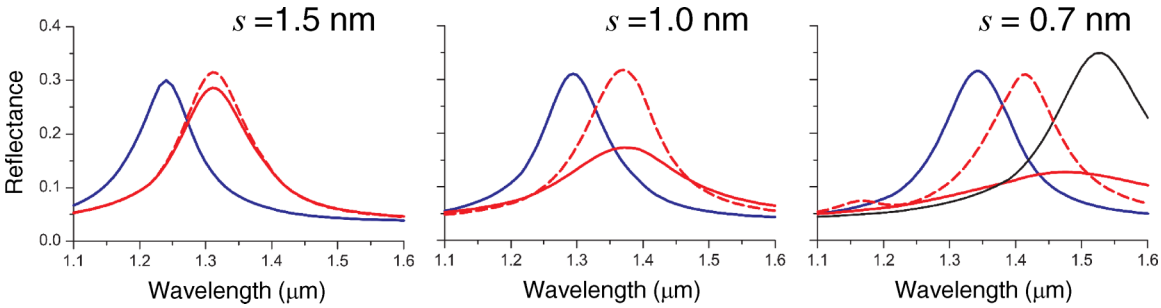

FIG. 4. The effect of the water layer in the gap between nanorods on the plasmon modes of the structure. Reflectance spectra of the periodic nanodolmen array with vacuum gap ($\varepsilon_g = 1.0$) is shown with blue lines; results obtained when the water layer is present in the gap are shown with red color. Dashed line: only dielectric properties of the water are accounted for ($\varepsilon_g = 1.8$). Solid line: dielectric screening and tunneling through water layer are accounted for with ε_g given by Eq. (4). Three panels of the figure correspond to the calculations performed with different size of the gap s as indicated. The reflectance spectra of fully metallic Π-type structure is shown with a black line on the right panel $s = 0.7$ nm.

TABLE I. The bulk refractive index sensitivity $\mathcal{S}$, the figure of merit FOM, and the alternative figure of merit FOM*[65] extracted from the spectra shown in Fig. 4. The sensor characteristics have been determined for the case when only dielectric screening of water is taken into account with $\varepsilon_g = 1.8$ and for the case when both screening and tunneling are accounted for with ε_g given by Eq. (4). Results are presented for the two widths of the gap $s = 1$ nm and $s = 0.7$ nm.

Model	Width s, nm	FWHM μm	$\Delta\lambda$ μm	S μm RIU^{-1}	FOM RIU^{-1}	FOM* RIU^{-1}
$\varepsilon_g = 1.8$	1	0.15	0.075	0.22	1.46	1.26
Eq. (4)	1	0.21	0.08	0.235	1.11	1.67
$\varepsilon_g = 1.8$	0.7	0.15	0.07	0.2	1.33	1.67
Eq. (4)	0.7	0.34	0.135	0.395	1.16	2.14

harms possible sensing applications in the tunneling regime. The geometry of the gap appears thus as an essential parameter that determines the effect of electron tunneling on the optical response of plasmonic structure [50–53].

A remark is in order with respect to possible effects of the nonlocal screening. Because of the nonlocal screening, the plasmon induced charges are not sharply located at the geometrical surfaces of the metals, as implicit for classical calculations, but span some distance range around these surfaces [58,59]. Within the classical electromagnetic calculations, the nonlocal screening effects are often incorporated using the hydrodynamical model [19,60,61], and more advanced approaches are also available [62]. As far as the frequency shift of the plasmon modes is concerned, a major effect of the nonlocal screening for the noble metal surfaces is that the effective (physical) width of the gap appears to be by typically by 0.2 nm larger than the geometrical width of the gap [63,64]. This is while the conductivity is not rescaled. As follows from Fig. 4 the nonlocal correction would not strongly affect present results, particularly as far as the tunneling effects are concerned.

Let us now discuss the possible application of the structure for sensing. Indeed, the spectra presented in Fig. 4 show that the presence of some layers of water in the gaps of 46×46 nm^2 cross sections significantly alters the resonance in the reflectance spectra of the periodic nanodolmen array so that small quantities of water can be detected. As usually reported, we characterize our sensor by the bulk refractive index sensitivity $\mathcal{S}$ and the figure of merit (FOM). The sensitivity is defined as $\mathcal{S} = \Delta\lambda/\Delta n$, where $\Delta\lambda$ is the shift in wavelength produced by the variation of the refractive index Δn. The FOM is defined as FOM $= \mathcal{S}/\Gamma$, where Γ is the full width at half maximum of the plasmon resonance in reflectance spectrum. The sensor characteristics of our device are listed in Table I. As compared to the effect of the dielectric screening only, for the narrow gap $s = 0.7$ nm the tunneling improves the sensitivity. The FOM is however reduced because of the resonance broadening. While reducing the FOM, the broadening and intensity loss of the plasmon resonance associated with tunneling effect, allows to improve the alternative figure of merit FOM* introduced in Ref. [65]. FOM* can be defined as relative reflectance $\mathcal{R}$ change $\mathcal{R}^{-1}\Delta\mathcal{R}/\Delta n$ at given wavelength λ, which we set here as a resonance wavelength for the vacuum gap. Overall, the sensing characteristics of

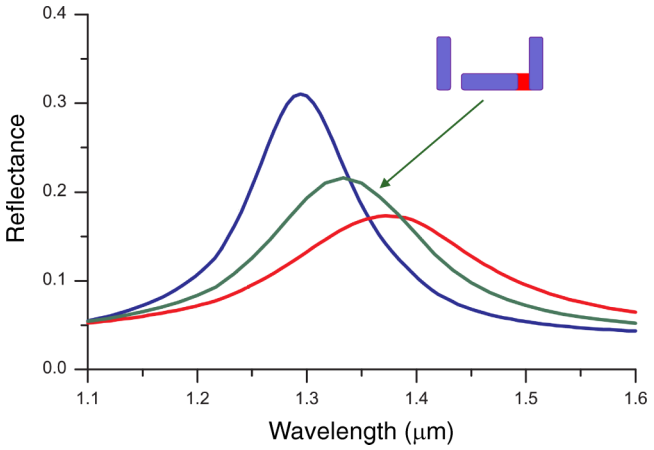

FIG. 5. The effect of the asymmetric filling of the gaps. Reflectance spectra of the periodic array formed by the nanodolmens with gap size $s = 1$ nm. Blue line: results obtained for the vacuum gaps. Green line: results obtained for one water and one vacuum gap as sketched in the figure. Red line: results obtained for water layer present in both gaps.

the periodic nanodolmen structure are comparable with other sensing devices reported in the literature [5,12,13]. It is worth it to stress here that in our design the index of refraction changes locally allowing us to probe the analyte at very low quantities. Moreover, electrically connecting nanorods similarly to the recently proposed electrically driven optical antenna design [66] and applying the dc bias might allow simultaneous measurement of the conductance and of the dielectric constant of the analyte.

Finally, we calculated the optical response of the structure for the case of asymmetric filling of the gaps. We suppose that only one gap is filled with water [ε_g is given by Eq. (4)], while the other one is characterized by the dielectric constant $\varepsilon_g = 1$. The comparison of the reflectance spectra of the nanostructure with vacuum gaps, water filled gaps, and one water and one vacuum gap is shown in Fig. 5 for the $s = 1$ nm case. The presence of water in only one junction reduces by nearly a factor of two the wavelength shift and broadening of the BP resonance as compared to the case where both plasmon gaps contain a water layer.

IV. SUMMARY AND CONCLUSIONS

In this study we have addressed the effect of the electron tunneling through the water layers in narrow gaps on the optical response of plasmonic nanostructures. The scanning tunneling microscopy measurements of the tunneling conductance of water allow parameter-free representation of the dielectric function of plasmonic gap that takes into account both dielectric screening and electron tunneling. With this representation, the optical properties of the system can be calculated using classical Maxwell equations. The methodology proposed here can be applied to any conductive medium in the junction, where the STM data can be used to predict the optical response.

With an example of the periodic array of gold nanodolmens we have demonstrated that the presence of water leads to the noticeable tunneling effects in plasmonic gaps of the widths of

1.5 nm and below. This range of the gap widths is substantially broader than that obtained in the estimations based on the vacuum tunneling junctions. Present results stem from the strong reduction of the electron tunneling barrier by the water layer present in the junction, as has been measured with STM and break junction techniques. Our conclusions are then robust and hold in general for plasmonic systems with narrow gaps. The comparison between vacuum and water junctions points at pronounced dependence of the observable quantum effects on the experimental conditions.

Along with the redshift of the bonding plasmon resonance because of the dielectric screening, the presence of water in nm gaps leads to the resonance broadening caused by the resistive losses associated with tunneling current. Both these effects can be used for the sensing applications of the structure, where quantum tunneling can improve sensing characteristics. Since we considered that water is present only in the gap region, *a priori* very small quantities of it can be detected. Electrically connecting the nanorods can provide further appealing perspectives, where the conductivity of the analyte can be measured simultaneously with measurement of the plasmon resonance shift.

While we studied the light scattering and absorption, another effect linked with interaction between tunneling electrons and photons has to be mentioned in connection with present results. As soon as tunneling through water or other conductive media, such as self-assembled molecular layers, is possible for the gap widths much larger than that for the vacuum gap, one expects that presence/absence of conductive media in the junction can have strong effect on the light emission triggered by the inelastic tunneling events [66–70].

Finally, the results obtained in this paper allow us to quantitatively address the effect of the presence of water on tunneling phenomena in plasmonics. This subject is of particular relevance owing to the intense theoretical and experimental activity aimed at description and understanding of the quantum effects in plasmonic response. Indeed, the theoretical quantum treatments reported so far consider vacuum gaps, while most of the experimental studies are performed in ambient conditions.

ACKNOWLEDGMENT

A.G.B. gratefully acknowledges the hospitality of the Donostia International Physics Center.

[1] J. A. Schuller, E. S. Barnard, W. Cai, Y. C. Jun, J. S. White, and M. L. Brongersma, Nat. Mater. **9**, 193 (2010).
[2] R. Alvarez-Puebla, L. M. Liz-Marzán, and F. J. García de Abajo, J. Phys. Chem. Lett. **1**, 2428 (2010).
[3] D. K. Gramotnev and S. I. Bozhevolnyi, Nat. Photon. **4**, 83 (2010).
[4] M. I. Stockman, Opt. Express **19**, 22029 (2011).
[5] M. E. Stewart, C. R. Anderton, L. B. Thompson, J. Maria, S. K. Gray, J. A. Rogers, and R. G. Nuzzo, Chem. Rev. **108**, 494 (2008).
[6] M. Rycenga, C. M. Cobley, J. Zeng, W. Li, C. H. Moran, Q. Zhang, D. Qin, and Y. Xia, Chem. Rev. **111**, 3669 (2011).
[7] Y. Wang, K. Sentosun, A. Li, M. Coronado-Puchau, A. Sánchez-Iglesias, S. Li, X. Su, S. Bals, and L. M. Liz-Marzán, Chem. Mater. **27**, 8032 (2015).
[8] N. J. Halas, S. Lal, S. Link, W. S. Chang, D. Natelson, J. H. Hafner, and P. Nordlander, Adv Mater. **24**, 4842 (2012).
[9] E. Hao and G. C. Schatz, J. Chem. Phys. **120**, 357 (2004).
[10] I. Romero, J. Aizpurua, G. W. Bryant, and F. J. García de Abajo, Opt. Express **14**, 9988 (2006).
[11] N. J. Halas, S. Lal, W.-S. Chang. S. Link, and P. Nordlander, Chem. Rev. **111**, 3913 (2011).
[12] K. M. Mayer and J. H. Hafner, Chem. Rev. **111**, 3828 (2011).
[13] J. Langer, S. M. Novikov, and L. M. Liz-Marzán, Nanotechnology **26**, 322001 (2015).
[14] P. K. Jain, W. Huang, and M. A. El-Sayed, Nano Lett. **7**, 2080 (2007).
[15] N. Liu, M. Hentschel, T. Weiss, A. P. Alivisatos, and H. Giessen, Science **332**, 1407 (2011).
[16] W. Cai, A. P. Vasudev, and M. L. Brongersma, Science **333**, 1720 (2011).
[17] M. Kauranen and A. V. Zayats, Nat. Photon. **6**, 737 (2012).
[18] D. C. Marinica, A. K. Kazansky, P. Nordlander, J. Aizpurua, and A. G. Borisov, Nano Lett. **12**, 1333 (2012).
[19] F. J. García de Abajo, J. Phys. Chem. C **112**, 17983 (2008).
[20] J. Zuloaga, E. Prodan, and P. Nordlander, Nano Lett. **9**, 887 (2009).
[21] P. Zhang, J. Feist, A. Rubio, P. García-González, and F. J. García-Vidal, Phys. Rev. B **90**, 161407(R) (2014).
[22] A. Varas, P. García-González, F. J. García-Vidal, and A. Rubio, J. Phys. Chem. Lett. **6**, 1891 (2015).
[23] T. P. Rossi, A. Zugarramurdi, M. J. Puska, and R. M. Nieminen, Phys. Rev. Lett. **115**, 236804 (2015).
[24] K. J. Savage, M. M. Hawkeye, R. Esteban, A. G. Borisov, J. Aizpurua, and J. J. Baumberg, Nature (London) **491**, 574 (2012).
[25] J. A. Scholl, A. García-Etxarri, A. L. Koh, and J. A. Dionne, Nano Lett. **13**, 564 (2013).
[26] H. Jung, H. Cha, D. Lee, and S. Yoon, ACS Nano **9**, 12292 (2015).
[27] G. Hajisalem, M. S. Nezami, and R. Gordon, Nano Lett. **14**, 6651 (2014).
[28] W. Zhu and K. B. Crozier, Nat. Commun. **5**, 5228 (2014).
[29] H. Cha, J. H. Yoon, and S. Yoon, ACS Nano **8**, 8554 (2014).
[30] R. Esteban, A. Zugarramurdi, P. Zhang, P. Nordlander, F. J. García-Vidal, A. G. Borisov, and J. Aizpurua, Faraday Discuss. **178**, 151 (2015).
[31] D. C. Marinica, M. Zapata, P. Nordlander, A. K. Kazansky, P. M. Echenique, J. Aizpurua, and A. G. Borisov, Science Advances **1**, e1501095 (2015).
[32] M. Hugelmann and W. Schindler, Surf. Sci. **541**, L643 (2003).
[33] J. R. Hahn, Y. A. Hong, and H. Kang, Appl. Phys. A **66**, S467 (1998).
[34] D.-H. Woo, E.-M. Choi, Y.-H. Yoon, K.-J. Kim, I. C. Jeon, and H. Kang, Surf. Sci. **601**, 1554 (2007).
[35] M. Heim, R. Eschrich, A. Hillebrand, H. F. Knapp, R. Guckenberger, and G. Cevc, J. Vac. Sci. Technol. B **14**, 1498 (1996).
[36] A. Mangin, A. Anthore, M. L. Della Rocca, E. Boulat, and P. Lafarge, Phys. Rev. B **80**, 235432 (2009).

[37] A. Stolz, J. Berthelot, M.-M. Mennemanteuil, G. Colas des Francs, L. Markey, V. Meunier, and A. Bouhelier, Nano Lett. **14**, 2330 (2014).
[38] B. Metzger, T. Schumacher, M. Hentschel, M. Lippitz, and H. Giessen, ACS Photonics **1**, 471 (2014).
[39] T. Coenen, D. T. Schoen, S. A. Mann, S. R. K. Rodriguez, B. J. M. Brenny, A. Polman, and M. L. Brongersma, Nano Lett. **15**, 7666 (2015).
[40] S. Biswas, J. Duan, D. Nepal, R. Pachter, and R. Vaia, Nano Lett. **13**, 2220 (2013).
[41] V. G. Kravets, F. Schedin, and A. N. Grigorenko, Phys. Rev. Lett. **101**, 087403 (2008).
[42] http://www.comsol.com.
[43] P. B. Johnson and R. Christy, Phys. Rev. B **6**, 4370 (1972).
[44] L. Olesen, M. Brandbyge, M. R. Sørensen, K. W. Jacobsen, E. Lægsgaard, I. Stensgaard, and F. Besenbacher, Phys. Rev. Lett. **76**, 1485 (1996).
[45] J. R. Tucker and M. J. Feldman, Rev. Mod. Phys. **57**, 1055 (1985).
[46] J. W. Haus, D. de Ceglia, M. A. Vincenti, and M. Scalora, JOSA B **31**, 259 (2014).
[47] I. Benjamin, D. Evans, and A. Nitzan, J. Chem. Phys. **106**, 6647 (1997).
[48] U. Peskin, Å. Edlund, I. Bar-On, M. Galperin, and A. Nitzan, J. Chem. Phys. **111**, 7558 (1999).
[49] C. S. Cucinotta, I. Rungger, and S. Sanvito, J. Phys. Chem. C **116**, 22129 (2012).
[50] H. Fischer and O. J. F. Martin, Opt. Express **16**, 9144 (2008).
[51] N. Grillet, D. Manchon, F. Bertorelle, C. Bonnet, M. Broyer, E. Cottancin, J. Lermé, M. Hillenkamp, and M. Pellarin, ACS Nano **5**, 9450 (2011).
[52] R. Esteban, G. Aguirregabiria, A. G. Borisov, Y. M. Wang, P. Nordlander, G. W. Bryant, and J. Aizpurua, ACS Photonics **2**, 295 (2015).
[53] D. Knebl, A. Hörl, A. Trügler, J. Kern, J. R. Krenn, P. Puschnig, and U. Hohenester, Phys. Rev. B **93**, 081405(R) (2016).
[54] W. Zhang and O. J. F. Martin, ACS Plasmonics **2**, 144 (2015).
[55] O. Pérez-González, N. Zabala, A. G. Borisov, N. J. Halas, P. Nordlander, and J. Aizpurua, Nano Lett. **10**, 3090 (2010).
[56] F. Benz, Ch. Tserkezis, L. O. Herrmann, B. de Nijs, A. Sanders, D. O. Sigle, L. Pukenas, S. D. Evans, J. Aizpurua, and J. J. Baumberg, Nano Lett. **15**, 669 (2015).
[57] S. Lerch and B. M. Reinhard, Adv. Mater. **28**, 2030 (2016).
[58] P. J. Feibelman, Prog. Surf Sci. **12**, 287 (1982).
[59] R. C. Monreal, T. J. Antosiewicz, and S. P. Apell, New J. Phys. **15**, 083044 (2013).
[60] A. I. Fernández-Domínguez, A. Wiener, F. J. García-Vidal, S. A. Maier, and J. B. Pendry, Phys. Rev. Lett. **108**, 106802 (2012).
[61] S. Raza, S. I. Bozhevolnyi, M. Wubs, and N. A. Mortensen, J. Phys. Condens. Matter **27**, 183204 (2015).
[62] W. Yan, M. Wubs, and N. Asger Mortensen, Phys. Rev. Lett. **115**, 137403 (2015).
[63] T. V. Teperik, P. Nordlander, J. Aizpurua, and A. G. Borisov, Phys. Rev. Lett. **110**, 263901 (2013).
[64] O. Schnitzer, V. Giannini, R. V. Craster, and S. A. Maier, Phys. Rev. B **93**, 041409(R) (2016).
[65] J. Becker, A. Trugler, A. Jakab, U. Hohenester, and C. Sonnichsen, Plasmonics **5**, 161 (2010).
[66] J. Kern, R. Kullock, J. Prangsma, M. Emmerling, M. Kamp, and B. Hecht, Nat. Photon. **9**, 582 (2015).
[67] M. G. Boyle, J. Mitra, and P. Dawson, Nanotechnology **20**, 335202 (2009).
[68] J. Lambe and S. L. McCarthy, Phys. Rev. Lett. **37**, 923 (1976).
[69] P. Johansson, R. C. Monreal, and P. Apell, Phys. Rev. B **42**, 9210 (1990).
[70] F. Rossel, M. Pivetta, and W.-D. Schneider, Surf. Sci. Rep. **65**, 129 (2010).